An unshakable carbon budget for the Himalaya

Lena Märki, Maarten Lupker, Christian France-Lanord, Jérôme Lavé, Sean Gallen, Ananta Gajurel, Negar Haghipour, Fanny Leuenberger-West, Timothy Eglinton

▶ **To cite this version:**

Lena Märki, Maarten Lupker, Christian France-Lanord, Jérôme Lavé, Sean Gallen, et al.. An unshakable carbon budget for the Himalaya. Nature Geoscience, 2021, 14, pp.745-750. 10.1038/s41561-021-00815-z . hal-03350217

HAL Id: hal-03350217
https://hal.science/hal-03350217v1

Submitted on 10 Oct 2022

HAL is a multi-disciplinary open access archive for the deposit and dissemination of scientific research documents, whether they are published or not. The documents may come from teaching and research institutions in France or abroad, or from public or private research centers.

L'archive ouverte pluridisciplinaire **HAL**, est destinée au dépôt et à la diffusion de documents scientifiques de niveau recherche, publiés ou non, émanant des établissements d'enseignement et de recherche français ou étrangers, des laboratoires publics ou privés.

An unshakable carbon budget for the Himalaya

Lena Märki *
Geological Institute, ETH Zürich, Switzerland
lena.maerki@alumni.ethz.ch

Maarten Lupker
Geological Institute, ETH Zürich, Switzerland
maarten.lupker@erdw.ethz.ch

Christian France-Lanord
Centre de Recherches Pétrographiques et Géochimiques, CNRS – Université de Lorraine, France
cfl@crpg.cnrs-nancy.fr

Jérôme Lavé
Centre de Recherches Pétrographiques et Géochimiques, CNRS – Université de Lorraine, France
jlave@crpg.cnrs-nancy.fr

Sean Gallen
Department of Geosciences, Colorado State University, Fort Collins, USA
sean.gallen@colostate.edu

Ananta P. Gajurel
Department of Geology, Tribhuvan University, Nepal
apgajurel@gmail.com

Negar Haghipour
Geological Institute, ETH Zürich, Switzerland
Ion Beam Physics, ETH Zürich, Switzerland
negar.haghipour@erdw.ethz.ch

Fanny Leuenberger-West
Geological Institute, ETH Zürich, Switzerland
lfanny@retired.ethz.ch

Timothy Eglinton
Geological Institute, ETH Zürich, Switzerland
timothy.eglinton@erdw.ethz.ch

An unshakable carbon budget for the Himalaya

Lena Märki[1], Maarten Lupker[1], Christian France-Lanord[2], Jérôme Lavé[2], Sean Gallen[3], Ananta P. Gajurel[4], Negar Haghipour[1,5], Fanny Leuenberger-West[1], Timothy Eglinton[1]

[1] Geological Institute, ETH Zürich, Zürich, Switzerland.

[2] Centre de Recherches Pétrographiques et Géochimiques (CRPG), CNRS – Université de Lorraine, Vandœuvre-lès-Nancy, France.

[3] Department of Geosciences, Colorado State University, Fort Collins, USA.

[4] Department of Geology, Tribhuvan University, Kathmandu, Nepal.

[5] Ion Beam Physics, ETH Zürich, Zürich, Switzerland.

The erosion and weathering of mountain ranges exert a key control on the long-term (10^5-10^6 yr) cycling of carbon between the Earth's surface and the crust. The net carbon budget of a mountain range reflects the co-existence of multiple carbon sources and sinks, with corresponding fluxes remaining difficult to quantify. Uncertain responses of these carbon fluxes due to the stochastic nature of erosional processes further complicates the extrapolation of short-term observations to longer, climatically relevant timescales. Here, we quantify the evolution of the organic and inorganic carbon fluxes in response to the 2015 Gorkha earthquake (Mw 7.8) in the Central Himalaya. We find that the Himalayan erosion acts as a net carbon sink mainly due to efficient biospheric organic carbon export. Our high-resolution time-series encompassing four monsoon seasons before and after the Gorkha earthquake, reveal that coseismic landslides did not significantly perturb large-scale Himalayan sediment and carbon fluxes. This muted response of the Central Himalaya to a geologically-frequent perturbation such as the Gorkha earthquake further suggests that our estimates are representative of at least interglacial timescales.

75 Mountain building and associated erosion are key players in the cycling of carbon
76 between the reservoirs of the Earth's surface and the crust, controlling the long-term evolution
77 of the global climate. The weathering of silicate minerals coupled to carbonate precipitation in
78 the oceans, as well as the erosion, riverine transport and burial of biospheric Organic Carbon
79 (OC) on continental margins represent major carbon sinks with respect to the Earth's surface[1,2].
80 While both mechanisms are enhanced in highly erosive environments such as the Himalaya[3–5],
81 their relative importance remains unclear. Enhanced silicate weathering rates associated with
82 the uplift of the Himalaya were initially suggested as the main driver of the global Cenozoic
83 cooling[6], but more recent work shows the importance of the organic pathway in the Himalayan
84 carbon budget[7,8].

85 Globally, these carbon sinks are counterbalanced by CO_2 emissions from volcanic activity
86 and metamorphic reactions, the latter constituting an important carbon source in the Central
87 Himalaya[9]. While these carbon sources are not directly related to erosion, other, yet poorly
88 constrained, mechanisms of carbon release during erosion have been identified. The oxidation
89 of rock-derived organic carbon[1,10] and sulfuric acid-mediated weathering of carbonate rocks[11]
90 have the potential to offset the previously mentioned carbon sinks[5]. Chemical weathering in
91 the Central Himalaya is dominated by the dissolution of carbonates[12], and it has been shown
92 that the sulfide oxidation coupled to carbonate weathering is likely an important carbon source
93 in this environment[12–14]. Defining the carbon budget of Himalayan erosion, therefore, requires
94 quantification and comparison of all of the above-mentioned sources and sinks.

95 While the carbon fluxes associated with the erosion of various mountain ranges have
96 been estimated[5,15], their integration over longer timescales remains challenging due to the

97 stochastic nature of erosional processes dominating sediment and solute fluxes in most
98 mountainous landscapes. This is especially important regarding the proposition that extreme
99 events such as earthquakes or floods could dominate the long-term budget of erosional carbon
100 fluxes[16,17]. Large earthquakes, coupled with coseismic landsliding, in particular, have been
101 shown to increase the riverine OC export[18,19], and fresh landslide scars can serve as loci for
102 enhanced chemical weathering rates of silicates and sulfide oxidation[20,21].

103 In the tectonically active Central Himalaya, major earthquakes are geologically-frequent
104 events with return times of 250-500 years[22]. As these events are still rare on an observational
105 timescale, their impact on the carbon budget of the Himalaya is unknown. In April 2015, the
106 Central Nepalese Himalaya was hit by the Mw 7.8 Gorkha earthquake and several strong to
107 major aftershocks[23]. The fault rupture caused > 25,000 coseismic landslides in the steep valleys
108 of the Upper Himalaya[24] (Fig. 1).

109 In this study, we assess the net carbon budget (organic and inorganic sources and sinks)
110 of erosion in the Narayani catchment in the Central Himalaya. Our set of daily suspended
111 sediment and water samples of the Narayani River during the monsoon seasons of a pre-
112 earthquake year (2010) and three years following the Gorkha earthquake (2015-2017) provides
113 a unique opportunity to evaluate the influence of such an extreme event on the carbon budget
114 of a large portion of the Himalaya. It also allows us to refine the carbon budget of Himalayan
115 erosion by evaluating the magnitude of the main carbon sinks and sources associated with the
116 erosion of the Himalaya.

117

Organic carbon export and chemical weathering time-series

With a catchment area of 32,000 km^2, the Narayani river basin covers around a third of the Nepalese Himalaya (Fig. 1). Our sampling station lies at the Himalayan front, near Narayanghat, shortly before the Narayani enters the Gangetic floodplain. The Indian Summer Monsoon (June-September) dominates the precipitation regime in the catchment and is responsible for around 80% of the annual water discharge[25]. The Narayani River annually exports around 100 Mt of sediments to the Gangetic floodplain (equivalent to ca. 1.6 mm/yr of erosion), around 95% of which is transported during the monsoon season[26,27]. The Gorkha earthquake, whose epicenter was located in the Narayani basin, heavily impacted the eastern part of the catchment with coseismic landslides, while the western part was mostly spared (Fig. 1). Coseismic landslides mobilized a total of ca. 0.20 ± 0.01 km^3 material in the Narayani catchment, which is around four times the interseismic annual volume of sediment yield of the Narayani, and equivalent to an average surface lowering over the entire catchment of ca. 6.3 ± 0.4 mm (Methods). The Narayani provides an ideal catchment area for studying the effect of such an extreme event at a scale large enough to be of global importance.

With our daily suspended sediment and water samples, we calculate the river suspended sediment yield, and the carbon fluxes linked to erosion of successive monsoon seasons. Records of total discharge and sediment yield ([27]; Department of Hydrology and Meteorology of Nepal (DHM); this study) of the Narayani from 8 years before the earthquake, reveal that the monsoon in 2015, which started shortly after the Gorkha earthquake, was particularly weak (Fig. 2). Despite the active coseismic landsliding in the catchment[24], the total sediment yield of the Narayani does not reveal a detectable earthquake signal and falls within

140 the observed trends before 2015. Sediment fluxes (relative to monsoon discharge), however,
141 peaked a year later. This peak in sediment yield is likely attributable to a delayed response to
142 the Gorkha earthquake and the reactivation or mobilization of landslide material that had not
143 previously connected to the fluvial network[24]. However, this high sediment yield disappears in
144 2017 despite an equally intense monsoon. As landslide rates have been shown to decay to
145 background values in 1-4 years after a large earthquake[28], we interpret that the Gorkha
146 earthquake signal dissipated by 2017.

147 To constrain the fluxes of biospheric OC (OC_{bio}, fresh OC derived from soils and plant
148 debris) export, we measured the total organic carbon (TOC) content and the radiogenic (^{14}C)
149 isotopic compositions of OC in riverine suspended sediment samples (Methods). The TOC
150 content of the suspended sediments from the Narayani varies between 0.04 and 0.99 % and the
151 fraction modern (Fm) of the OC spans a large range, varying between 0.27 and 0.91 (Extended
152 Data Fig. 3). Our high-resolution time-series (with measurements up to every second day)
153 reveal a large variability in TOC concentrations and ^{14}C signatures of suspended sediments. For
154 disentangling the OC_{bio} and petrogenic OC (OC_{petro}, rock-derived OC) inputs, we employ a binary
155 mixing model using the TOC and the radiocarbon signatures of the bulk samples as well as a
156 biospheric and a petrogenic end-member (Methods and Extended Data Fig. 3). Soil samples
157 from the Narayani catchment mostly reflect a recent biospheric endmember (Fm 1.1 – 0.9),
158 whereas the petrogenic end-member was assigned an Fm value of 0. Hydrodynamic processes
159 do not significantly affect OC concentrations within the water column in large and turbulent
160 Himalayan river systems[29], including the Narayani (Supplementary Information). We can,
161 therefore, confidently assume that suspended sediment samples collected from surface waters

are representative of the OC_{bio} content in the whole water column. Using the measured daily sediment load and discharge data from the DHM, we are able to estimate the total amount of OC_{bio} exported by the Narayani River during a monsoon season and upscale it to a year (Methods).

Major ion concentrations measured in filtered river water (every day for the monsoon 2010; every second day for monsoons 2015-2017) provide estimates for silicate and carbonate weathering rates by carbonic and sulfuric acid, respectively. We calculate the relative amounts of silicate and carbonate weathering using a forward Monte Carlo approach with known elemental ratios of the weathering products of the main lithologies of the Central Himalaya[12,13] (Methods). We consider the CO_2 removal over timescales >10^4 yr for which one mole of carbon is removed from the Earth's surface through carbonate precipitation per mole of Ca and Mg derived from silicate weathering by carbonic acid[2] (Ca_{sil} and Mg_{sil}). The carbon source through carbonate weathering by sulfuric acid is calculated using the SO_4^{2-} concentration and the known ratio of carbonate to silicate weathering (Methods). In Himalayan rivers, the proportion of SO_4^{2-} derived from sulfide oxidation has been estimated to 60-100% ([12,14]). Per mole of carbonates weathered by sulfuric acid, half a mole of carbon is released to the atmosphere on timescales of 10^5-10^7 yr ([11]).

To complement our analysis of the carbon budget of Himalayan erosion, we estimate the OC_{petro} oxidation rate in the Narayani basin with Rhenium (Re) data from the literature. Dissolved Re concentrations serve as a proxy to trace the fluxes of carbon released through rock-derived carbon oxidation[10,30]. Compiling Re concentrations of Himalayan rivers and sediments[30–33] allows us to provide a first-order estimate of the carbon flux released through

184 OC_{petro} oxidation in the Central Himalaya (Methods). It should, however, be noted that these
185 estimates do not allow us to derive annually resolved OC_{petro} oxidation fluxes estimates since Re
186 was not directly measured in our samples.

187

188 **Carbon fluxes over four monsoon seasons**

189 The fraction of OC_{bio} in the total sediment load of the Narayani is diluted with increasing
190 runoff (Fig. 3a), which has been proposed to result from a lower degree of soil erosion relative
191 to mass wasting during the monsoon[27]. At higher discharge the concentration of OC_{bio} remains
192 constant despite changing runoff, which suggests that the OC_{bio} is supply-limited, similar to the
193 total sediment load in the Narayani[26,27]. The slightly higher concentrations of OC_{bio} in the year
194 2015 could be associated with material evacuated from coseismic landslides or could
195 alternatively be linked to the lower sediment load during this weak monsoon season. The
196 unusually large sediment yield observed in 2016 (Fig. 4a) is accompanied by a substantially
197 higher OC_{bio} export compared to the other years on record (Fig. 4b). This ca. 85% increase in
198 OC_{bio} export (Source Data Fig. 4) combined with a ca. 130% higher than expected sediment yield
199 (from the linear relationship between the total discharge and the monsoonal sediment yield,
200 Fig. 2) is likely a delayed manifestation of the coseismic landslides associated with the Gorkha
201 earthquake. However, this earthquake signal in the total sediment and the OC_{bio} export 2016 of
202 the Narayani disappears a year later, suggesting that significant portions of the landslide
203 sediments are either not or only very slowly evacuated.

As reported in previous studies, our results show that chemical weathering in the Central Himalaya is dominated by carbonates, with around 10% of the cations being derived from silicate weathering[12,34,35]. The calculated Ca_{sil} and Mg_{sil} concentrations do not significantly vary between the different years (Fig. 3b). The concentration of SO_4^{2-} coupled with carbonate weathering, displays a typical dilution pattern that has been described for anion concentrations in the Himalaya[12,35] (Fig. 3d). When summing up these carbon fluxes per monsoon season (Fig. 4c and 4d), we observe that the carbon source through sulfuric acid weathering is ~2.5 times higher than the carbon sink through silicate weathering, which lies in the same order of magnitude as recently proposed[14]. Both of these carbon fluxes did not significantly increase after the Gorkha earthquake at the scale of the Narayani basin.

Minor earthquake impact on the Himalayan carbon budget

Our data suggest that, in contrast to other seismically impacted systems, the Central Himalaya had a muted response to the Gorkha earthquake. The Mw 7.9 earthquake that struck Wenchuan in 2008 resulted in widespread coseismic landsliding[36], increased riverine sediment fluxes[37] and doubled OC_{bio} export over four years after the earthquake[18]. Similar to the Narayani, the catchment studied after the Wenchuan earthquake was only partly affected by coseismic landslides (0.14 and 0.27% ([37]) of the respective catchment areas). Furthermore, sediment cores from a mountain lake in the Southern Alps of New Zealand revealed that over the last ~1000 yr large earthquakes were responsible for 27% of the sediment flux[38] and 43% of the OC_{bio} export[19] in its catchment.

225 Despite similar moment magnitudes, the coseismic landslides after Wenchuan
226 earthquake mobilized a substantially larger volume of material (~2.3 km^3 ([36])) than the total
227 landsliding associated with the Gorkha earthquake (~0.8 km^3 ([24])). In addition, the landslide
228 density in the Central Himalaya during the year 2015 was only 4-6 times higher relative to that
229 during interseismic periods[39]. This increase in landslide density following the Gorkha
230 earthquake was significantly lower than the 22 times higher landslide density in the year after
231 an earthquake of similar strength in 1999 in Taiwan[28]. While the relatively weak earthquake
232 impact on landsliding rates in the Central Himalaya can partly be linked to the seismic rupture
233 characteristics[40], the short major earthquake recurrence[22] and high density of interseismic
234 landsliding[39] result in a landscape that is in quasi-equilibrium with frequent mass wasting. The
235 addition of coseismic landslide material equivalent to around four years of interseismic erosion
236 in the Narayani catchment was therefore likely not sufficient to significantly perturb the
237 geochemical fluxes in this highly erosive system. The magnitude of a perturbation relative to
238 background conditions exerts thus an important influence on the system's response.

239 Earthquakes with a larger moment magnitude than the Mw 7.8 Gorkha earthquake
240 trigger more landslides[36] but the long recurrence-time of great (Mw >9) earthquakes in the
241 Himalaya, which is on the order millennia[41], means that they do not dominate the long-term
242 erosion budget[39]. We similarly assume that long-term carbon fluxes associated with erosion
243 processes in the Central Himalaya would not be significantly impacted by larger and less
244 frequent earthquakes compared to Gorkha.

245

The net carbon budget of the Central Himalayan erosion

Integrating the mean carbon fluxes at the Himalayan outlet constrained for four years reveals that the Central Himalayan erosion acts as a net carbon sink with respect to the Earth's surface (Fig. 4e). Due to relatively low interannual variability and stability with respect to seismic perturbations, we propose that these Himalayan carbon fluxes are representative for long-term periods with relatively stable climatic conditions, such as interglacials. The magnitude of carbon removal through OC_{bio} export (and subsequent burial) is around ten times larger than the sink resulting from silicate weathering (and subsequent carbonate precipitation). This finding further underlines the predominant role of the organic carbon cycle in the Himalaya[7,8]. Moreover, our results demonstrate that the relative contribution of OC_{bio} export versus silicate weathering to the carbon sink at the outlet of the Himalaya is higher than previously found in Neogene sediments of the Bay of Bengal[7,42]. As highlighted for other mountain ranges[5], the oxidative weathering of OC_{petro} and sulfuric acid weathering of carbonates are important carbon sources that must be included in the net carbon budget of the Himalayan erosion. The comparison of the OC_{petro} oxidation flux with the calculated riverine export of OC_{petro} suggests that ca. 36% of the total OC in the bedrock is lost to oxidation within the catchment (Supplementary Information). This oxidation rate remains lower than that previously calculated for Taiwan[43].

Overall, these results provide additional insights into the erosional carbon budget of a tectonically active and highly erosive mountain range. We emphasize that carbon fluxes were calculated for the outlet of the Himalayan front, from where the solutes and sediments transit through the Gangetic floodplain before being discharged in the Bay of Bengal. It has been

shown that Himalayan OC_{bio} is oxidized and replaced during floodplain transit[8]. Nevertheless, the constant OC concentration of sediments during transport and the high OC burial efficiency in the Bay of Bengal[42] imply that the OC burial flux is unaffected by floodplain transfer. In contrast, chemical weathering rates have been shown to double from the Himalayan front to the Indian Ocean[13,44]. Further weathering of carbonates by sulfuric acid during floodplain transfer is probably small given that sulfides oxidize readily upon exposure at the surface in the upland areas[14,45] and are not detected in the sediment load downstream in the Gangetic floodplain[46]. At the same time, oxidation rates of rock-derived OC are likely to increase in the Ganges by 50-70% ([47]). Hence, while some of the carbon fluxes likely increase during the transport through the Gangetic floodplain, the overall carbon budget from the Central Himalaya is unlikely to be significantly shifted in one direction.

This unique time-series dataset from before and after the 2015 Gorkha earthquake allows us to evaluate the impact of an extreme event on the carbon fluxes of the Central Himalayan erosion. Unlike previously studied systems[18,19], Himalayan carbon fluxes were not significantly perturbed by a major earthquake. This budget reveals that the erosion of a large Himalayan catchment acts as a net carbon sink, although this sink is smaller than previously thought[6–8] and reflects the complex interplay of processes that must be considered in developing net erosional carbon budgets. Due to relatively low interannual variability, Himalayan carbon fluxes can be integrated on timescales of at least interglacials. While the export and burial rates of OC_{bio}, as well as chemical weathering rates in the Ganges-Brahmaputra basin, both fluctuate on glacial-interglacial timescales[48,49], it has recently been

shown that erosion rates in this basin remained relatively stable during the late Cenozoic[50]. As erosion exerts a primary control on carbon fluxes[5], we speculate that our carbon budget for the Central Himalaya may be relevant on late Cenozoic timescales representing a long-term net carbon sink.

Data availability

All data analyzed in this study are available in the Research Collection of ETH Zurich at http://hdl.handle.net/20.500.11850/487683.

References

1. Berner, R. A. & Canfield, D. E. A new model for atmospheric oxygen over Phanerozoic time. *Am. J. Sci.* **289**, 333–361 (1989).

2. Walker, J. C. G., Hays, P. B. & Kasting, J. F. A negative feedback mechanism for the long-term stabilization of Earth's surface temperature. *J. Geophys. Res. Ocean.* **86**, 9776–9782 (1981).

3. West, A. J. Thickness of the chemical weathering zone and implications for erosional and climatic drivers of weathering and for carbon-cycle feedbacks. *Geology* **40**, 811–814 (2012).

4. Galy, V., Peucker-Ehrenbrink, B. & Eglinton, T. Global carbon export from the terrestrial biosphere controlled by erosion. *Nature* **521**, 204–207 (2015).

5. Hilton, R. G. & West, A. J. Mountains, erosion and the carbon cycle. *Nat. Rev. Earth Environ.* **1**, 284–299 (2020).

6. Raymo, M. E. & Ruddiman, W. F. Tectonic forcing of late Cenozoic climate. *Nature* **357**, 57–59 (1992).

7. France-Lanord, C. & Derry, L. A. Organic carbon burial forcing of the carbon cycle from Himalayan erosion. *Nature* **390**, 65–67 (1997).

8. Galy, V., France-Lanord, C. & Lartiges, B. Loading and fate of particulate organic carbon from the Himalaya to the Ganga-Brahmaputra delta. *Geochim. Cosmochim. Acta* **72**, 1767–1787 (2008).

9. Evans, M. J., Derry, L. A. & France-Lanord, C. Degassing of metamorphic carbon dioxide from the Nepal Himalaya. *Geochemistry, Geophys. Geosystems* **9**, (2008).

10. Hilton, R. G., Gaillardet, J., Calmels, D. & Birck, J. L. Geological respiration of a mountain belt revealed by the trace element rhenium. *Earth Planet. Sci. Lett.* **403**, 27–36 (2014).

11. Calmels, D., Gaillardet, J., Brenot, A. & France-Lanord, C. Sustained sulfide oxidation by physical erosion processes in the Mackenzie River basin: Climatic perspectives. *Geology* **35**, 1003–1006 (2007).

12. Galy, A. & France-Lanord, C. Weathering processes in the Ganges-Brahmaputra basin and the riverine alkalinity budget. *Chem. Geol.* **159**, 31–60 (1999).

13. Bickle, M. J. *et al.* Chemical weathering outputs from the flood plain of the Ganga. *Geochim. Cosmochim. Acta* **225**, 146–175 (2018).

14. Kemeny, P. C. *et al.* Sulfate sulfur isotopes and major ion chemistry reveal that pyrite oxidation counteracts CO2 drawdown from silicate weathering in the Langtang-Trisuli-Narayani River system , Nepal Himalaya. *Geochim. Cosmochim. Acta* **294**, 43–69 (2021).

15. Horan, K. *et al.* Carbon dioxide emissions by rock organic carbon oxidation and the net geochemical carbon budget of the Mackenzie River Basin. *Am. J. Sci.* **319**, 473–499 (2019).

16. Hilton, R. G. *et al.* Tropical-cyclone-driven erosion of the terrestrial biosphere from mountains. *Nat. Geosci.* **1**, 759–762 (2008).

17. Wang, J. *et al.* Long-term patterns of hillslope erosion by earthquake-induced landslides shape mountain landscapes. *Sci. Adv.* **6**, https://doi.org/10.1126/sciadv.aaz6446 (2020).

18. Wang, J. *et al.* Earthquake-triggered increase in biospheric carbon export from a mountain belt. *Geology* **44**, https://doi.org/10.1130/G37533.1 (2016).

19. Frith, N. V *et al.* Carbon export from mountain forests enhanced by earthquake-triggered landslides over millennia. *Nat. Geosci.* **11**, 772–776 (2018).

20. Emberson, R., Hovius, N., Galy, A. & Marc, O. Chemical weathering in active mountain belts controlled by stochastic bedrock landsliding. *Nat. Geosci.* **9**, 42–45 (2016).

21. Emberson, R., Galy, A. & Hovius, N. Weathering of Reactive Mineral Phases in Landslides Acts as a Source of Carbon Dioxide in Mountain Belts. *J. Geophys. Res. Earth Surf.* **123**, 2695–2713 (2018).

22. Avouac, J. P., Bollinger, L., Lave, J., Cattin, R. & Flouzat, M. Seismic cycle in the Himalayas.

Comptes Rendus l'Academie Sci. - Ser. IIa Sci. la Terre des Planetes **333**, 513–529 (2001).

23. Avouac, J.-P., Meng, L., Wei, S., Wang, T. & Ampuero, J.-P. Lower edge of locked Main Himalayan Thrust unzipped by the 2015 Gorkha earthquake. *Nat. Geosci.* **8**, 708–711 (2015).

24. Roback, K. *et al.* The size, distribution, and mobility of landslides caused by the 2015 Mw7.8 Gorkha earthquake, Nepal. *Geomorphology* **301**, 121–138 (2018).

25. Andermann, C. *et al.* Impact of transient groundwater storage on the discharge of Himalayan rivers. *Nat. Geosci.* **5**, 127–132 (2012).

26. Andermann, C., Crave, A., Gloaguen, R. & Davy, P. Connecting source and transport : Suspended sediments in the Nepal Himalayas. *Earth Planet. Sci. Lett.* **352**, 158–170 (2012).

27. Morin, G. P. *et al.* Annual Sediment Transport Dynamics in the Narayani Basin, Central Nepal: Assessing the Impacts of Erosion Processes in the Annual Sediment Budget. *J. Geophys. Res. Earth Surf.* **123**, 2341–2376 (2018).

28. Marc, O., Hovius, N., Meunier, P., Uchida, T. & Hayashi, S. Transient changes of landslide rates after earthquakes. *Geology* **43**, 883–886 (2015).

29. Menges, J. *et al.* Variations in organic carbon sourcing along a trans-Himalayan river determined by a Bayesian mixing approach. *Geochim. Cosmochim. Acta* **286**, 159–176 (2020).

30. Dalai, T. K., Singh, S. K., Trivedi, J. R. & Krishnaswami, S. Dissolved rhenium in the Yamuna

River System and the Ganga in the Himalaya: Role of black shale weathering on the budgets of Re, Os, and U in rivers and CO2 in the atmosphere. *Geochim. Cosmochim. Acta* **66**, 29–43 (2002).

31. Rahaman, W., Singh, S. K. & Shukla, A. D. Rhenium in Indian rivers: Sources, fluxes, and contribution to oceanic budget. *Geochemistry, Geophys. Geosystems* **13**, (2012).

32. Paul, M. (Université de Lorraine). Etude des isotopes de l'osmium dans les eaux souterraines du Bangladesh et les sédiments himalayens: implications et rôle de l'érosion himalayenne sur le budget océanique de l'osmium. (2018).

33. Pierson-Wickmann, A. C., Reisberg, L. & France-Lanord, C. The Os isotopic composition of Himalayan river bedloads and bedrocks: Importance of black shales. *Earth Planet. Sci. Lett.* **176**, 203–218 (2000).

34. France-Lanord, C., Evans, M., Hurtrez, J. E. & Riotte, J. Annual dissolved fluxes from Central Nepal rivers: Budget of chemical erosion in the Himalayas. *Comptes Rendus - Geosci.* **335**, 1131–1140 (2003).

35. Bhatt, M. P., Hartmann, J. & Acevedo, M. F. Seasonal variations of biogeochemical matter export along the Langtang-Narayani river system in central Himalaya. *Geochim. Cosmochim. Acta* **238**, 208–234 (2018).

36. Marc, O., Hovius, N., Meunier, P., Gorum, T. & Uchida, T. A seismologically consistent expression for the total area and volume of earthquake-triggered landsliding. *J. Geophys. Res. Earth Surf.* https://doi:10.1002/2015JF003732 (2016).

37. Wang, J. *et al.* Controls on fluvial evacuation of sediment from earthquake-triggered landslides. *Geology* **43**, 115–118 (2015).

38. Howarth, J. D., Fitzsimons, S. J., Norris, R. J. & Jacobsen, G. E. Lake sediments record cycles of sediment flux driven by large earthquakes on the Alpine fault , New Zealand. *Geology* **40**, 1091–1094 (2012).

39. Marc, O. *et al.* Long-term erosion of the Nepal Himalayas by bedrock landsliding: The role of monsoons, earthquakes and giant landslides. *Earth Surf. Dyn.* **7**, 107–128 (2019).

40. Xu, C. *et al.* Two Comparable Earthquakes Produced Greatly Different Coseismic Landslides : The 2015 Gorkha , Nepal and 2008 Wenchuan, China Events. *J. Earth Sci.* **27**, 1008–1015 (2016).

41. Stevens, V. L. & Avouac, J. P. Millenary Mw > 9.0 earthquakes required by geodetic strain in the Himalaya. *Geophys. Res. Lett.* **43**, 1118–1123 (2016).

42. Galy, V. *et al.* Efficient organic carbon burial in the Bengal fan sustained by the Himalayan erosional system. *Nature* **470**, 407–411 (2007).

43. Hemingway, J. D. *et al.* Microbial oxidation of lithospheric organic carbon in rapidly eroding tropical mountain soils. *Science* **360**, 209–212 (2018).

44. Lupker, M. *et al.* Predominant floodplain over mountain weathering of Himalayan sediments (Ganga basin). *Geochim. Cosmochim. Acta* **84**, 410–432 (2012).

45. Torres, M. A. *et al.* The acid and alkalinity budgets of weathering in the Andes–Amazon system: Insights into the erosional control of global biogeochemical cycles. *Earth Planet.*

410 *Sci. Lett.* **450**, 381–391 (2016).

411 46. Garzanti, E. *et al.* Mineralogical and chemical variability of fluvial sediments 2 .
412 Suspended-load silt (Ganga-Brahmaputra, Bangladesh). *Earth Planet. Sci. Lett.* **302**, 107–
413 120 (2011).

414 47. Galy, V., Beyssac, O., France-Lanord, C. & Eglinton, T. Recycling of graphite during
415 Himalayan erosion: a geological stabilization of carbon in the crust. *Science* **322**, 943–945
416 (2008).

417 48. Lupker, M., France-Lanord, C., Galy, V., Lavé, J. & Kudrass, H. Increasing chemical
418 weathering in the Himalayan system since the Last Glacial Maximum. *Earth Planet. Sci.*
419 *Lett.* **365**, 243–252 (2013).

420 49. Hein, C. J. *et al.* Post-glacial climate forcing of surface processes in the Ganges –
421 Brahmaputra river basin and implications for carbon sequestration. *Earth Planet. Sci.*
422 *Lett.* **478**, 89–101 (2017).

423 50. Lenard, S. J. P. *et al.* Steady erosion rates in the Himalayas through late Cenozoic climatic
424 changes. *Nat. Geosci.* **13**, 448–452 (2020).

425

426 **Acknowledgments**

427 L.M., M.L. and T.E. were supported by the Swiss National Science Foundation (No.
428 200021_166067). C. F.-L. and J.L. were supported by the ANR Calimero. We thank K. B. Adhikari
429 from the hydrological station in Narayanghat for the daily sampling. E. Tipper (University of

Cambridge) is thanked for kindly providing the confluence samples. We further thank J. Wang, K. Clark and an anonymous Reviewer for their constructive comments on the manuscript.

Author contributions

L.M. and M.L. designed the study. M.L., C. F.-L., J.L., A.G. and S.G. organized and maintained daily sampling in Narayanghat. J.L. provided the depth profile samples and L.M., M.L., C.F-L., J.L. and S.G. conducted the soil sampling. L.M., N.H. and F.W.-L. prepared the samples and preformed the measurements. S.G. conducted the landslide volume calculation. L.M., M.L. and T.E. made the carbon flux calculations. All authors contributed to the interpretation of the data and the redaction of the manuscript.

Competing interests

The authors declare no competing interests.

Corresponding author

Correspondance and requests for materials can be addressed to Lena Märki (lena.maerki@alumni.ethz.ch).

Figure captions

Fig. 1: Map of the Central Himalaya and location of the studied drainage basin. *The Narayani catchment (dashed outline) and the sampling station in Narayanghat are displayed. The epicenter of the 2015 Gorkha earthquake is shown by the star, and red dots illustrate the mapped coseismic landslides[24]. The topographic map is from Hydrosheds (http://hydrosheds.cr.usgs.gov).*

Fig. 2: Total water discharge and sediment yield of the Narayani River during different monsoon seasons. *River during different monsoon seasons. Total discharge as a function of the sediment yield of the monsoon months June-July-August-September (JJAS) of the Narayani in Narayanghat (discharge data and sediment loads from 2001-2012 from the Department of Hydrology and Meteorology of Nepal and ref.[27]). Uncertainty on the sediment export is reported as 10% of the estimated value to account for the depth correction of the surface sediment load[27] and uncertainties on water discharge reported by the Department of Hydrology and Meteorology of Nepal are unknown but likely smaller than the symbol. Dashed lines illustrate the 0.997 confidence interval of the linear regression between discharge and sediment yield. Grey points show records after the April 2015 Gorkha earthquake.*

Fig. 3: OC_{bio}, Ca_{sil}+Mg_{sil} and $SO_4^{2-}{}_{carb}$ as a function of the discharge of the Narayani River. a. *Biospheric organic carbon (OC_{bio}) as weight percent of the total suspended sediment. Literature data are from ref.[8] (pre-earthquake). The typical error bar includes the 10% uncertainty in the total sediment yield[27] and the standard deviation of the*

OC_{bio} apportionment calculation. ***b.*** *Concentrations of Ca and Mg derived from silicate weathering through carbonic acid (Ca_{sil}+Mg_{sil}). Literature data are from refs.*[12,34,35] *(pre-earthquake) and ref.*[13] *(post-earthquake). The reported typical error is associated to the systematic uncertainty (standard deviation) in the silicate apportionment of Ca and Mg fluxes and the end-member Ca_{sil} and Mg_{sil} elemental ratios.* ***c.*** *Concentration of the fraction of SO_4^{2-} associated with carbonate weathering ($SO_4^{2-}{}_{carb}$). Literature data are from refs.*[12,34,35] *(pre-earthquake) and ref.*[13] *(post-earthquake). The typical error bar illustrates the 30% uncertainty due to the proportion of SO_4^{2-} which is derived from sulfide oxidation*[12,14]*. Panels a, b and c are plotted against the daily water discharge of the Narayani River in Narayanghat provided by the Department of Hydrology and Meteorology of Nepal.*

Fig. 4: Total carbon fluxes and mean net erosional carbon budget for the Narayani basin through four monsoon seasons. *Total export during four monsoon seasons of* ***a.*** *suspended sediments (error bars indicate 10% error due to the depth correction of the surface sediment load*[27]*);* ***b.*** *OC_{bio} (error bars include uncertainty in the total sediment yield and the standard deviation of the OC_{bio} calculation from total OC);* ***c.*** *Ca_{sil} + Mg_{sil} (for the errors the standard deviation of the elemental ratios defining Ca_{sil} and Mg_{sil} are propagated); and* ***d.*** *$SO_4^{2-}{}_{carb}$ (error bars indicate the range of 100-70% of SO_4^{2-} which is derived from sulfide oxidation*[12,14]*). Round symbols illustrate the Gorkha earthquake that happened shortly before the monsoon 2015.* ***e.*** *Mean carbon fluxes from the four studied years of erosion in the Narayani basin in t of C/(km^2yr) and in moles of C/(km^2yr). Total fluxes in tC/(km^2yr) and in tC/yr are indicated in square brackets. Error bars are calculated by the mean of the above-described errors, and for*

the OC_{petro} oxidation, the error of the oxidation rate calculation is propagated (see also Methods). Red bar illustrates the sum of the carbon fluxes, and its error bar is propagated with a Monte Carlo simulation.

Methods

Calculation of coseismic landslide volume and lowering rates

The total volume of coseismic landslide material in the Narayani catchment was calculated using the earthquake-triggered landslide inventory from ref.[24] and the area-volume scaling parameters from ref.[51] (Extended Data Table 1). We here used the global parameters from ref.[51]. The uncertainties were propagated with a Monte Carlo approach ($n = 10^4$). The mean landscape surface lowering rate was obtained by dividing the landslide volume within the catchment by the Narayani catchment surface area (32,000 km^2).

Sampling

Surface suspended sediments were taken in the middle of the Narayani river during the monsoon seasons (June-September) 2010 and 2015-2017 (Source Data Fig. 3). The sampling in 2010 is described in more detail in ref.[27] and is similar to the sampling during the other years. For samples in 2015-2017, 3L of surface water was taken at the sampling station in Narayanghat (27.73° N; 84.43° E). The water was immediately filtered with a pressure filtration unit through 0.2 µm polyethersulfone (PES) membranes, and the sediment sample was stored

512 in a dark and cool place until return to the laboratory. 250 ml of the filtered river water was
513 collected for measurements of major ions.

514 Sediment sampling of four depth profiles (Source Data Extended Data Fig. 4) within the
515 water column was performed in 2011 in Narayanghat and is further described in ref.[27]. At the
516 sampling location, the Narayani channel is around 15-20 m deep. Samples of both tributaries
517 shortly before the confluence, which is situated around 2 km upstream of the sampling station
518 and samples from both sides of the Narayani river, were taken during different field campaigns
519 between 2015 and 2017 (Source Data Extended Data Fig. 5). For the samples NEQ-17204 - NEQ-
520 172-39, 10-20L of surface water was filtered as described above and stored in a cool place.
521 Samples NEP-15-02 – NEP-17-43 were taken with a bucket or a sediment sampler from the
522 surface water and filtered through a pressure filtration unit similar as described above.

523 Soil samples (Extended Data Table 2) cover a variety of conditions such as elevation and
524 annual precipitation within the Narayani catchment and were collected between 2009 and
525 2017. The samples are further described in ref.[52]. The samples integrate the surface soil layer of
526 a depth of up to 15 cm. The uppermost few cm of the soils were removed for not including
527 vegetation and litter in the surface soil samples.

528

529 **Determination of the total sediment yield of a monsoon season**

530 Out of the 488 studied days, for 28 days the sediment load was not measured and was
531 therefore estimated based on water discharge. For estimating the missing sediment load data,
532 we applied the method described in ref.[27]. Briefly, a digital filter[53] was used to separate the

533 total discharge of the Narayani in the baseflow and the direct discharge[26] with the parameters
534 used in ref.[27] (Extended Data Fig. 1). The missing sediment load was subsequently calculated
535 with the linear regression between the direct discharge and the sediment load data (Extended
536 Data Fig. 2).

537 **TOC, $\delta^{13}C$ and radiocarbon measurement of suspended sediments**

538 Sediment and soil samples were frozen upon arrival at ETH Zürich and subsequently
539 freeze-dried. Sediments were weighed for calculating the surface sediment load and carefully
540 removed from the filters. Soil samples were sieved at < 2 mm. An aliquot of the sediments and
541 soils was milled in a Retsch zirconium ball mill. ~50 mg of the milled samples were weighed into
542 combusted silver capsules. Samples were fumigated in HCl vapor for removal of inorganic
543 carbon (3 days at 60 °C), and neutralized with NaOH (4 days at 60 °C). The capsules were
544 subsequently wrapped in tin boats, and TOC and its isotopic compositions were measured on a
545 coupled online elemental analyzer-isotope ratio mass spectrometer-accelerator mass
546 spectrometer (EA-IRMS-AMS) system[54] at the Ion Beam Physics Institute of the ETH Zürich.
547 $^{13}C/^{12}C$ ratios are reported in $\delta^{13}C$ notation relative to the Vienna Pee Dee Belemnite (VPDB)
548 standard and the ^{14}C content is reported as fraction modern (Fm).

549 In addition to routine standard measurements by AMS[54], an internal standard consisting
550 of a suspended sediment sample was measured eight times in different batches (including
551 different fumigation batches). The standard deviation of the results is used as typical
552 uncertainty on the measurements (TOC: mean 0.24% ± 0.01; Fm: mean 0.51 ± 0.03; $\delta^{13}C$: mean
553 -24.02 ‰ ± 0.17).

554

555 **Determination of OC_{bio} yield**

556 A binary mixing model was applied to disentangle the concentrations of OC_{bio} and OC_{petro}
557 ($[OC_{bio}]$ and $[OC_{petro}]$) in the total OC of the suspended sediment (Extended Data Fig. 3). With
558 the following assumptions similar to the method applied in ref.[43] we are able calculate the
559 concentrations (%) of OC_{bio} and OC_{petro} in the total sediment:

560 $$[OC_{tot}] = [OC_{bio}] + [OC_{petro}] \quad (1)$$

561 $$Fm_{tot} * [OC_{tot}] = Fm_{bio} * [OC_{bio}] + Fm_{petro} * [OC_{petro}] \quad (2)$$

562 The rock-derived OC_{petro} is characterized by $Fm_{petro} = 0$ because its age exceeds the ^{14}C half-life
563 by more than an order of magnitude. We can therefore rewrite equations 1 and 2:

564 $$Fm_{tot} * [OC_{tot}] = Fm_{bio} * [OC_{bio}] \quad (3)$$

565 $$[OC_{bio}] = [OC_{tot}] - [OC_{petro}] \quad (4)$$

566 If we combine the equations we obtain:

567 $$Fm_{tot} * [OC_{tot}] = Fm_{bio} * ([OC_{tot}] - [OC_{petro}]) \quad (5)$$

568 From where we can calculate $[OC_{petro}]$

569 $$[OC_{petro}] = [OC_{tot}] - (Fm_{tot} * [OC_{tot}]) / Fm_{bio} \quad (6)$$

570 And $[OC_{bio}]$

571 $$[OC_{bio}] = [OC_{tot}] - [OC_{petro}] \quad (7)$$

572 The radiocarbon signature of 17 surface soils from the Narayani basin (Extended Data
573 Table 2) was used to define the Fm of the OC_{bio} endmember (Fm_{bio} = 1.1- 0.9). OC_{tot} and Fm_{tot}
574 are the measured values, and standard deviations are derived from the internal standard as
575 described above. A Monte Carlo simulation ($n=10^5$) was used to randomly sample within the
576 Fm_{bio} endmember and the standard deviation of OC_{tot} and Fm_{tot}. Errors of the model were
577 defined by the standard deviation of the model results. This approach for determining OC_{bio} is
578 not as sensitive to possible autocorrelation biases as previous studies[47]. In the latter study, the
579 OC_{petro}, was determined by the intersection of the linear correlation between the TOC and the
580 value of TOC*Fm. This method and the calculations done in our study, however, give broadly
581 similar results.

582 In order to calculate the total sediment yield, the surface sediment load was corrected
583 for increasing concentrations with the depth of the water column. For this purpose, we use the
584 method proposed by ref.[27] (equation 3.2), which integrates the surface sediment concentration
585 for depth and water velocity in the Narayani river. The daily discharge data of the Narayani river
586 was provided by the Department of Hydrology and Meteorology of Nepal (DHM), enabling
587 calculation of daily sediment yield of the Narayani during the four studied monsoon seasons.
588 With these data we were able to calculate the total amount of OC_{bio} exported by the Narayani
589 in a given day for which TOC and Fm measurements are available. We observe a high daily
590 variability in our TOC and Fm data without any significant correlation to the runoff, the
591 sediment load or the season at the time of sampling. We upscale the estimate to the entire
592 monsoon and hence interpolate across days without TOC and Fm measurements as follows:

593 $\Sigma[OC_{bio}(measured)]$ * Σdaily sediment yield (all) / Σdaily sediment yield (with Fm and TOC
594 measurement)

595 The concentration of TOC and its radiocarbon signature of surface sediments is taken to
596 be representative of the whole water column (Supplementary Information and Extended Data
597 Fig. 4). Suspended sediment samples from upstream the major confluence close to the
598 sampling station confirm that incomplete mixing of the sediments from this confluence does
599 not have a major influence on the TOC and radiocarbon concentration in Narayanghat
600 (Supplementary Information and Extended Data Fig. 5).

601

602 **Chemical weathering rates calculated by major ion chemistry**

603 The concentrations of major cations in water samples from 2010 were determined with
604 an Inductively Coupled Plasma Optical Emission Spectroscopy (ICP-OES) at the CRPG Nancy.
605 Major cations and anions of samples from 2015-2017 were measured by Ion Chromatography
606 (IC) at ETH Zürich. All results are reported in the Source Data Fig. 3. Ion concentrations were
607 corrected for atmospheric input, as suggested by ref.[12] and using ion concentrations of
608 rainwater from ref.[55]. Concentrations of Cl and SO_4 for the year 2010 were estimated by
609 correlating the concentrations of the measured years to river discharge (Supplementary
610 Information and Extended Data Fig. 6 and 7).

611 Concentrations of Ca and Mg derived from silicate weathering through carbonic acid
612 (Ca_{sil} and Mg_{sil}) were calculated using elemental ratios of silicates and carbonates in the Central

613 Himalaya from refs.[12,13]. A Monte Carlo simulation (n=10^5) sampled randomly within a normal
614 distribution with the following standard deviation.

615 Mg_{sil} = K * x ; x=0.5 with standard deviation of 0.25 (ref.[12]) (8)

616 Ca_{sil} = (Na-Cl) * y ; y=0.4 with standard deviation of 0.15 (ref.[13]) (9)

617 The proportion of silicate weathering relative to carbonate weathering (x_{sil}) was calculated:

618 X_{sil} = (1.8 * (Na – Cl) + 2* K) / (Na + K + 2*Mg + 2* Ca) (modified from ref.[12]) (10)

619 All the concentrations in equations 8-12 have been corrected for atmospheric input.

620 Secondary calcite precipitation along the Narayani and its tributary might slightly bias x_{sil}
621 ([13,56]), but at the scale of the whole catchment, we assume that its effect is minor. For the years
622 2015-2017, where every second day was measured, the days without measurement had to be
623 interpolated for the calculation of total fluxes per monsoon. Interpolation was done by taking
624 the average of the measurements from the day before and after. This method takes into
625 account previously reported seasonal changes of weathering rates and dilution effects in the
626 beginning of the monsoon season[12,56]. Using the daily discharge data from the DHM we are able
627 to calculate the total flux of Ca_{sil} and Mg_{sil} per monsoon.

628 For calculating the long-term carbon sink through silicate weathering, we subtract the
629 amount of Ca_{sil} and Mg_{sil} derived from sulfuric acid weathering as the latter does not involve
630 any carbon uptake. We here assume that sulfuric acid reacts with carbonates and silicates in
631 the same relative proportions as carbonic acid[57]. As the chemical weathering regime of the
632 Himalaya is dominated by carbonates[12], we notice that the hypothesis that sulfuric acid only

633 weathers carbonate minerals would not have a significant effect on our total carbon flux
634 calculations.

635 We can use x_{sil}:

636 $$SO_{4,sil} = SO_{4,tot} * x_{sil} \quad (11)$$

637 We define the proportion of Mg and Ca in the total ions derived from silicate weathering:

638 $$(Mg_{sil} + Ca_{sil})_{SO4} = SO_{4,sil} * ((Ca_{sil} + Mg_{sil}) / (Ca_{sil} + Mg_{sil} + K/2 + (Na\text{-}Cl) /2) \quad (12)$$

639 where Na-Cl is the total Na derived from silicate weathering[12]. We then calculate the Mg_{sil} and
640 Ca_{sil} that has been weathered through carbonic acid.

641 $$(Mg_{sil} + Ca_{sil})_{HCO3} = (Mg_{sil} + Ca_{sil})_{tot} – (Mg_{sil} + Ca_{sil})_{SO4} \quad (13)$$

642 Finally, one mole of carbon per mole of $Ca_{sil,HCO3}$ or $Mg_{sil,HCO3}$ can be removed from the
643 Earth's surface through carbonate precipitation and is thus considered as a long-term (>10^5 yr)
644 carbon sink. As cation exchange between sediments and seawater is negligible[58] we do not take
645 into account K and Na for the long-term carbon removal through silicate weathering.

646 For determining the proportion of carbonates weathered by sulfuric acid we can modify
647 equation 11:

648 $$SO_{4,carb} = SO_{4,tot} * (1\text{-}x_{sil}) \quad (14)$$

649 The main uncertainty of the sulfuric acid weathering rate calculation derives from the
650 unknown proportion of SO_4^- derived from evaporites. The latter produces SO_4^- during
651 weathering but does not produce sulfuric acid which could act as a weathering agent. Previous

studies estimate the evaporitic input in the Narayani basin as negligible to up to 40% of the total SO_4^- ([12,14]). We, therefore, use error bars between 100 – 70% for the calculated values. For calculating total fluxes per monsoon, we use the same interpolation as described above for silicate weathering.

OC_{petro} oxidation calculation with dissolved Re

The release of carbon through OC_{petro} oxidation in the Narayani catchment was estimated using Re as a tracer for the weathering of OC_{petro} [10,30,59]. This gives us a first-order estimation of the magnitude of the carbon flux linked to OC_{petro} oxidation but does not allow us to account for annual differences of this carbon flux. We compiled dissolved Re and major cations concentration data from global rivers[10,15,30,31,59,60]. While the total dataset displays a relatively weak linear correlation between the sum of cations and the Re concentration (r^2 = 0.41), Himalayan rivers show a strong linear relationship as suggested earlier[31] (r^2 = 0.83) (Extended Data Fig. 8). We calculate the mean flux of dissolved Re (Re_{flux}, 40.7 kg/monsoon) over the four studied monsoon seasons based on the regression between Re and total cation concentrations obtained from all Himalayan rivers. A Monte Carlo simulation ($n=10^5$) sampled randomly within a normal distribution in the one-sigma confidence interval of the regression for estimating a mean Re concentration for each studied monsoon season based on the mean annual sum of cations. Data of Re concentrations in bulk suspended sediments from the Narayani from refs.[32,33] (Re_{sd}; 2.7-4.8 * 10^{-10} pg/g) are used together with the mean OC_{petro}

concentration of samples from this study (OC_{sd}). The OC_{petro} oxidation rate is finally calculated as described in ref.[59] with a Monte Carlo simulation ($n=10^5$):

$$C_{released} = Re_{flux} * (OC_{sd}/Re_{sd}) * f_C - f_{graphite} \quad (15)$$

Where f_c is the factor correcting for Re from inorganic phases and for the ratio of Re dissolved during OC_{petro} oxidation in soils ($0.5 < f_c < 1$; [10,59,61] and $f_{graphite}$ corrects for the fraction of crystalline graphite that is less prone to oxidation ($0.3 < f_{graphite} < 0.5$; estimated from data from ref.[47]).

Upscaling from a monsoonal to an annual carbon budget

The erosion as well as the carbon fluxes in the Central Himalaya, are mostly driven by the monsoonal precipitation. In order to render our carbon flux calculations comparable to other studies, we up-scale the monsoonal carbon budget to annual values based on the following assumptions. For the total OC_{bio} export we considered that ~95% of the annually suspended sediments of the Narayani are discharged during the monsoon[26] and that the relative importance of soil erosion increases during the dry season[27]. We, therefore, assume that the OC_{bio} discharged during the monsoon represents 90% of the annual OC_{bio} export. The monsoonal total OC and OC_{petro} export is assumed to follow the total sediment flux constituting 95% of the annual flux. For the silicate weathering budget, we follow ref.[56] who showed that in the Central Himalaya, ~60% of the annual silicate weathering flux is occurring during the monsoon. As the monsoon accounts for ~80% of the total water discharge of the Narayani River[26], we assume this same proportion for carbonate weathering by sulfuric acid and OC_{petro}

693 oxidation. This calculation is conservative, as the fraction of sulfuric acid relative to carbonic
694 acid is likely decreasing during the monsoon in the headwaters of the Narayani[56].

695 **References Methods**

696 51. Larsen, I. J., Montgomery, D. R. & Korup, O. Landslide erosion controlled by hillslope
697 material. *Nat. Geosci.* **3**, 247–251 (2010).

698 52. Märki, L. *et al.* Molecular tracing of riverine soil organic matter from the Central
699 Himalaya. *Geophys. Res. Lett.* **47**, https://doi.org/10.1029/2020GL087403 (2020).

700 53. Eckhardt, K. How to construct recursive digital filters for baseflow separation. *Hydrol.*
701 *Process.* **19**, 507–515 (2005).

702 54. McIntyre, C. P. *et al.* Online 13C and 14C Gas Measurements by EA-IRMS–AMS at ETH
703 Zürich. *Radiocarbon* **59**, 893–903 (2017).

704 55. Wolff-Boenisch, D., Gabet, E. J., Burbank, D. W., Langner, H. & Putkonen, J. Spatial
705 variations in chemical weathering and CO2 consumption in Nepalese High Himalayan
706 catchments during the monsoon season. *Geochim. Cosmochim. Acta* **73**, 3148–3170
707 (2009).

708 56. Tipper, E. T. *et al.* The short term climatic sensitivity of carbonate and silicate weathering
709 fluxes: Insight from seasonal variations in river chemistry. *Geochim. Cosmochim. Acta* **70**,
710 2737–2754 (2006).

711 57. Burke, A. *et al.* Sulfur isotopes in rivers : Insights into global weathering budgets, pyrite
712 oxidation, and the modern sulfur cycle. *Earth Planet. Sci. Lett.* **496**, 168–177 (2018).

713 58. Lupker, M., France-Lanord, C. & Lartiges, B. Impact of sediment-seawater cation
714 exchange on Himalayan chemical weathering fluxes. *Earth Surf. Dyn.* **4**, 675–684 (2016).

59. Horan, K. *et al.* Mountain glaciation drives rapid oxidation of rock-bound organic carbon. *Sci. Adv.* **3**, https://doi.org/10.1126/sciadv.1701107 (2017).

60. Miller, C. A., Peucker-Ehrenbrink, B., Walker, B. D. & Marcantonio, F. Re-assessing the surface cycling of molybdenum and rhenium. *Geochim. Cosmochim. Acta* **75**, 7146–7179 (2011).

61. Pierson-Wickmann, A. C., Reisberg, L. & France-Lanord, C. Behavior of Re and Os during low-temperature alteration: Results from Himalayan soils and altered black shales. *Geochim. Cosmochim. Acta* **66**, 1539–1548 (2002).

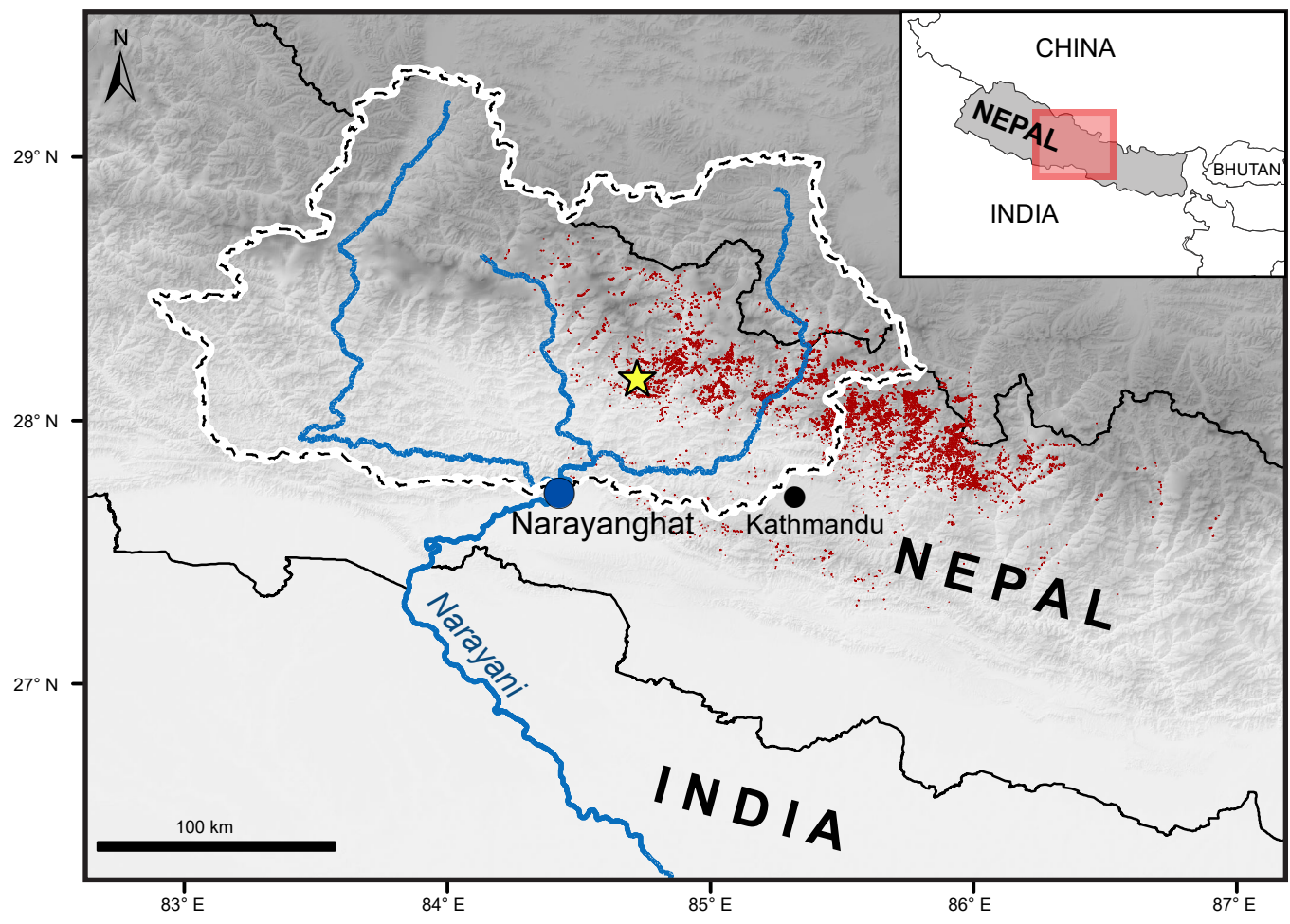
N
29° N
28° N
27° N
83° E
84° E
85° E
86° E
87° E
CHINA
NEPAL
BHUTAN
INDIA
Narayanghat
Kathmandu
NEPAL
Narayani
INDIA
100 km

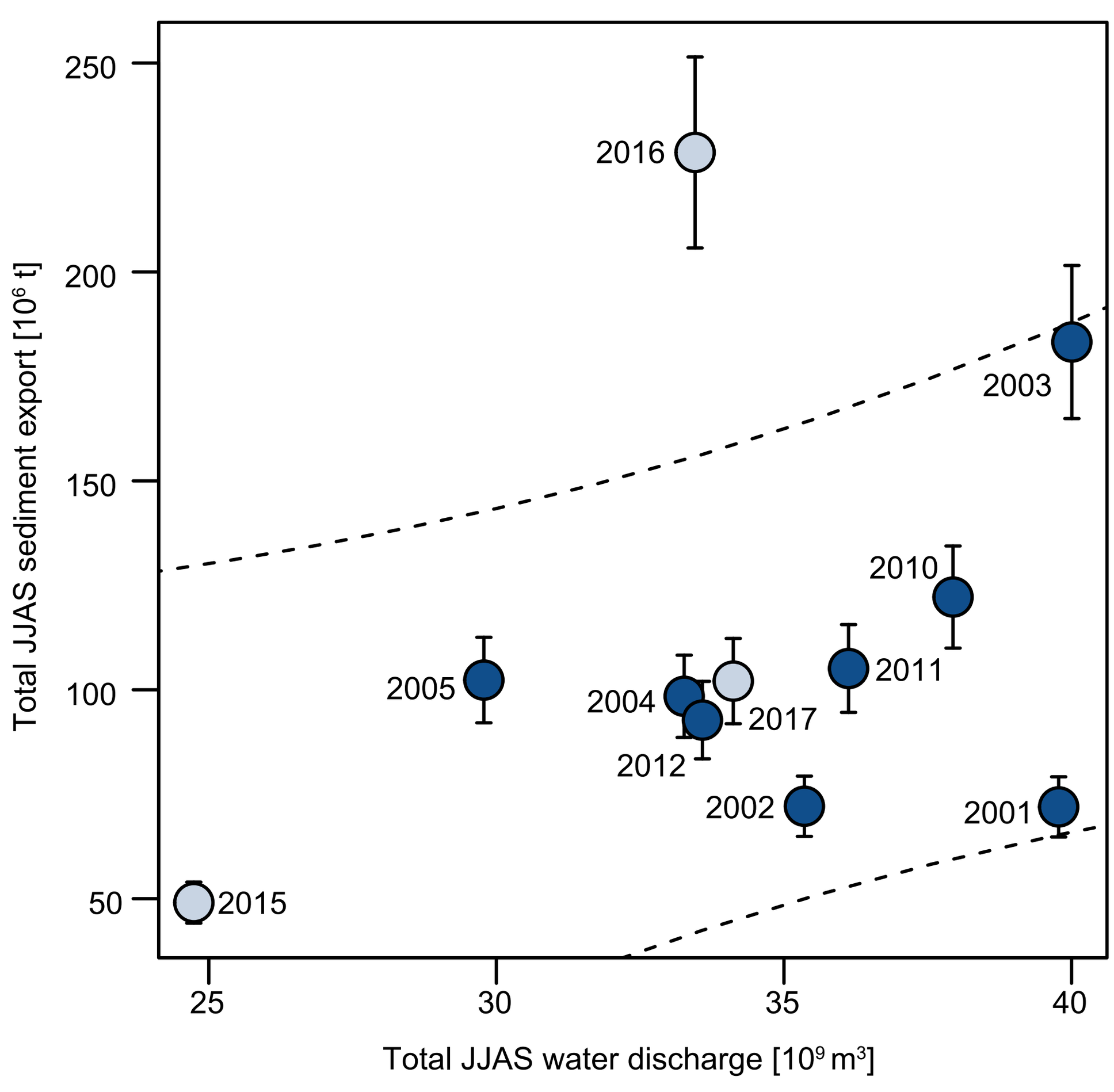
250
200
150
100
50
Total JJAS sediment export [10^6 t]
2016
2003
2010
2005
2004
2017
2011
2012
2002
2001
2015
25
30
35
40
Total JJAS water discharge [10^9 m^3]

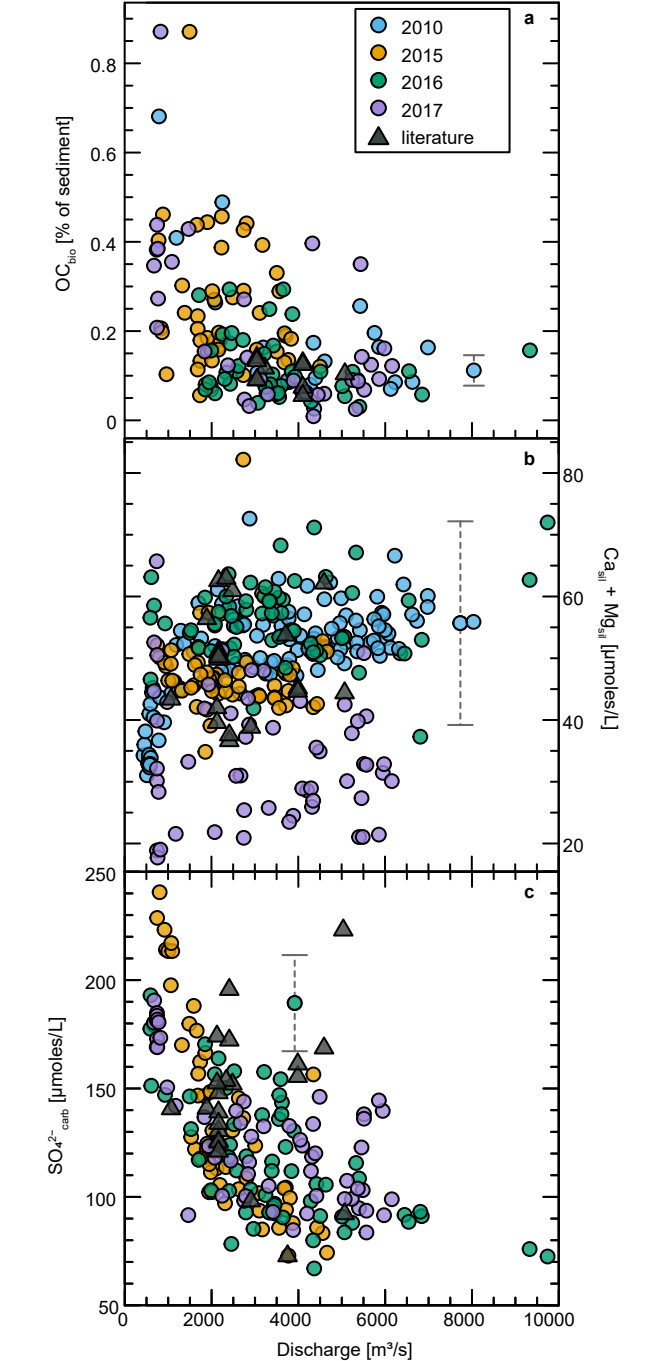
a
b
c
2010
2015
2016
2017
literature
OC_{bio} [% of sediment]
$Ca_{sil} + Mg_{sil}$ [µmoles/L]
$SO_4^{2-}{}_{carb}$ [µmoles/L]
Discharge [m³/s]
0
0.2
0.4
0.6
0.8
20
40
60
80
50
100
150
200
250
2000
4000
6000
8000
10000

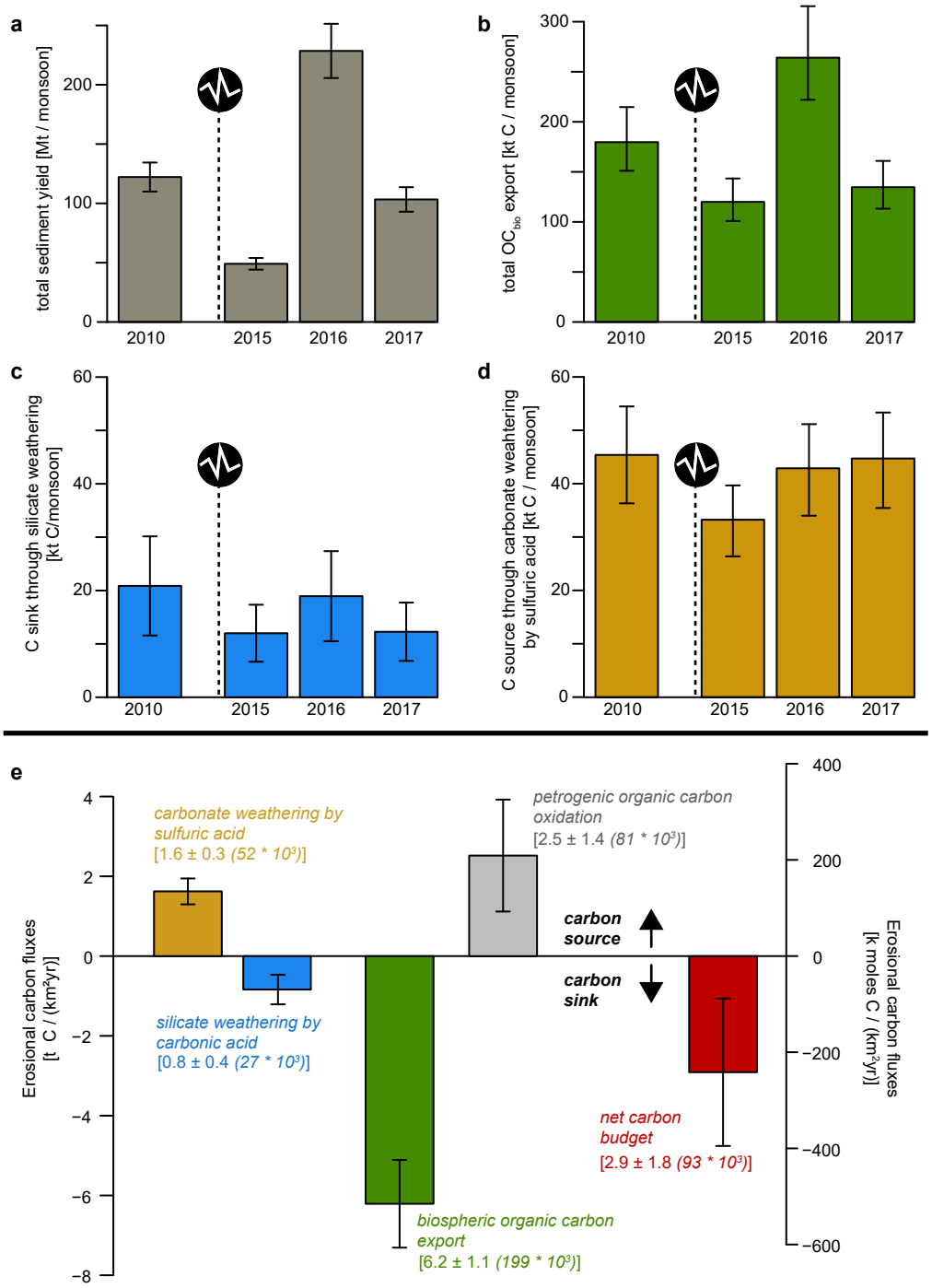
a
total sediment yield [Mt / monsoon]
0
100
200
2010
2015
2016
2017
b
total OC_{bio} export [kt C / monsoon]
0
100
200
300
2010
2015
2016
2017
c
C sink through silicate weathering [kt C/monsoon]
0
20
40
60
2010
2015
2016
2017
d
C source through carbonate weahtering by sulfuric acid [kt C / monsoon]
0
20
40
60
2010
2015
2016
2017
e
Erosional carbon fluxes [t C / (km²yr)]
4
2
0
−2
−4
−6
−8
Erosional carbon fluxes [k moles C / (km²yr)]
400
200
0
−200
−400
−600
carbonate weathering by sulfuric acid [1.6 ± 0.3 (52 * 10³)]
silicate weathering by carbonic acid [0.8 ± 0.4 (27 * 10³)]
petrogenic organic carbon oxidation [2.5 ± 1.4 (81 * 10³)]
carbon source
carbon sink
biospheric organic carbon export [6.2 ± 1.1 (199 * 10³)]
net carbon budget [2.9 ± 1.8 (93 * 10³)]